Power constrained NCS design for SIMO plant models

Alejandro Rojas[1] and Héctor Ramírez[2]

***Abstract*— In this article, we investigate a networked control system (NCS) in which the feedback path is implemented via a set of parallel additive white noise (AWN) channels subject to an aggregate power constraint. The plant under consideration has a single input and multiple outputs, i.e., it is a single-input multi-output (SIMO) system. Such a SIMO configuration may arise, for example, when actuators are significantly more expensive than sensors, or when a single physical process is instrumented with spatially distributed sensing devices, as in the case of water canal systems. The controller synthesis is carried out in discrete time, which is particularly suitable for NCS implementations; however, the methodology can be extended to the continuous-time domain without conceptual difficulties. The resulting control design guarantees closed-loop stability for a given input power over the communication channels, subject to the structural constraints imposed by the SIMO plant model.**

I. INTRODUCTION

Automatic Control Theory can be traced back to foundational developments in the nineteenth century, followed by a marked growth in research activity in the second half of the twentieth century, which produced well-established results such as the Proportional–Integral–Derivative (PID) controller [1], the Linear Quadratic Regulator (LQR), and the Kalman filter. These and other contributions constitute what is now regarded as classical automatic control theory; see, for example, [2]. The practical application of automatic control theory is commonly referred as control engineering [3], a discipline that has played a pivotal role in disseminating and embedding automatic control principles across nearly all engineering domains. Reciprocally, the requirements and constraints imposed by real-world systems have stimulated the advancement of novel theoretical methodologies.

At the turn of the twenty-first century, the classical paradigm of closed-loop feedback in automatic control was revised through the explicit incorporation of information transmission processes. This integration of automatic control, information theory, and communication theory gave rise to the field of Networked Control Systems (NCS). In comparison with traditional automatic control, NCS has enabled a substantially broader range of applications [4], including the characterization of new fundamental limitations [5], [6], as well as advances in consensus control and multi-agent system coordination.

*This work was supported by grants ANID Fondecyt Regular 1230777 and ANID AC3E CIA250006.

[1]Alejandro Rojas is with the Department of Electrical Engineering, Universidad de Concepción, Concepción, Chile `arojasn@udec.cl`

[2]Héctor Ramírez is with the Department of Electronic Engineering, Universidad Técnica Federico Santa María, Valparaíso, Chile `hector.ramireze@usm.cl`

The main components of any NCS, namely communication, computation, and control, are reviewed in [7] for distributed processes within the framework of three methodological perspectives: (i) undirected and directed graph representations, (ii) fixed and time-varying network topologies, and (iii) event-triggered control mechanisms. In contrast, a control-over-network perspective for spatially distributed NCS in [8] identifies five major research directions: sampled-data control, quantized control, networked control, event-triggered control, and security-oriented control. Markov jump linear system theory is employed in [9] to design delay-free error-correction codes for control over networks with packet erasures, ensuring closed-loop stability whenever at least k output symbols are received, and guaranteeing a prescribed performance level if the average number of received symbols exceeds k. In [10], uncertainties are modeled in terms of plant perturbations, transmission delays, and fading channels, and the problem is formulated as an NCS stabilization task. A stabilizing controller is first synthesized for the nominal NCS, and subsequently extended to a robust controller under the prescribed uncertainties, using symmetric matrix homogeneous polynomials whose feasibility is verified via Linear Matrix Inequalities (LMIs). As an application, a parallel transmission strategy is proposed, and the corresponding maximum allowable delay uncertainty is derived as an explicit function of the nominal plant model parameters and the channel input signal-to-noise ratio (SNR).

When the plant is modeled as a single-input multi-output (SIMO) system, it can, for example, represent a dam–river configuration, as in [11], where the overall dynamics are described by a series of interconnected single-input single-output (SISO) subsystems. In this setting, intermediate water-level measurements provide an approximation of the underlying spatially distributed dynamics of a physical river. The spatial separation inherent in such systems necessitates explicit communication to transmit the water-level measurements to an upstream controller, which subsequently computes the appropriate water discharge. A water-canal network thus constitutes a canonical example of a NCS. One class of NCSs involves communication over an additive white noise (AWN) channel subject to a channel input SNR constraint.

The article [12] examines the optimal tracking performance for a SIMO system, where the dominant communication impairment is modeled as the rate of transmitted packet dropouts. In that work, the optimal controller is determined by searching over the entire set of stabilizing controllers. Furthermore, [13] analyzes the performance of a SIMO NCS in the presence of network-induced delays. In this

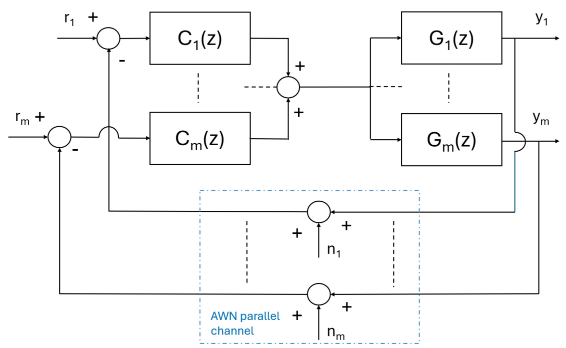

Fig. 1. NCS based on a set of AWN parallel channel over the feedback path.

case, an inner–outer factorization approach combined with a two-degrees-of-freedom (2-DOF) controller architecture is employed. The attainable control performance has also been characterized as a function of the unstable poles and non-minimum phase zeros of the plant model. In [14], SIMO NCS error performance is investigated under the combined effects of transmission quantization and packet dropouts, and in [15] for repeated plant model poles and zeros. The optimal tracking error performance is derived in the frequency domain, and it is shown to depend on the locations of the plant poles and zeros, as well as on communication-related properties such as quantization characteristics and packet dropout rate. Finally, the minimal SNR for the scalar communication channel is studied for SIMO systems in [16].

The contribution of this work is in the research area of distributed NCS, specifically for SIMO systems. Here we provide an SNR stability bound for a SIMO NCS, over a feedback path set of parallel AWN channel models, see Fig. 1. The required channel inputs power constraints are achieved for a discrete time controller that take into accounts the plant unstable poles and the structural limitation imposed by the SIMO structure, while ensuring closed feedback loop stability. Asymptotic tracking performance is then achieved with a 2 DOF controller structure. The channel input power constraint will then be equivalently stated, when all the additive channel noises share the same variance value, as an overall channel input SNR.

This article has the following structure: Section II present the required preliminary knowledge required to state the contributed results. In Section III we develop the channel input power result and the related SIMO controller design that achieves it. The equivalent SNR characterization will also be presented here. In Section IV we provide examples to further gain insight from the contributed results. We then close this article with our final remarks and future research directions in Section V.

II. Preliminaries

In this section we introduce the details about the closed feedback loop in Fig. 1, as well as the assumptions for the AWN parallel channel. We also state the SNR problem to be solved in the next section.

- **SIMO plant model:** The SIMO plant model under study is defined as

$$G(z) = \begin{bmatrix} G_1(z) & \cdots & G_m(z) \end{bmatrix}^T \tag{1}$$

where each plant model is in turn defined as $G_i(z) = \frac{k_i}{z-\rho_i} G_{si}(z)$, ρ_i real number, $|\rho_i| > 1$, $\rho_i \neq \rho_j$ if $i \neq j$, and each $G_{si}(z)$ is a stable, minimum phase, biproper transfer function, for $i = 1, \cdots, m$. Each plant model captures the dominant unstable dynamic for each parallel feedback loop, and group the rest of the stable dynamics in the term $G_{si}(z)$. The distinct poles requirement is without loss of generality, and it is in place to avoid overly complex expressions in the proposed analysis.

- **AWN parallel channel :** each AWN channel model is subject to a channel input power constraint $\mathcal{P}_i$. The channel additive noise n_i, $i = 1, \cdots, m$, is a zero mean, i.i.d. white noise process, which is also independent of the other channel noises. The variance of each additive channel noise is given by σ_i^2.

- **Controller model:** The controller model must be dimensionally compatible with the SIMO plant model. This results in a controller model with multi-inputs and a single-output (MISO), see Fig. 1. Each element of the overall controller is an LTI transfer function to be designed to solve the SNR problem , that is

$$C(z) = \begin{bmatrix} C_1(z) & \cdots & C_m(z) \end{bmatrix} \tag{2}$$

Furthermore, in general, and if not stated otherwise, we assume that each controller element is defined as $C_i(z) = k_{ci} G_{si}^{-1}(z)$, that is each controller inverts the stable, minimum phase and biproper part of their respective plant model element and introduces a gain parameter k_{ci}, to be designed, to achieve overall closed feedback loop stability and solve the SNR problem.

We now state the SNR problem for the closed feedback loop in Fig. 1, assuming all setpoint signals to be zero to study the regulation case. The closed loop relationship between the output vector signal $\mathbf{y} = \begin{bmatrix} y_1 & \cdots & y_m \end{bmatrix}^T$, and the channel noise vector $\mathbf{n} = \begin{bmatrix} n_1 & \cdots & n_m \end{bmatrix}^T$, , is defined as

$$\mathbf{y} = -T(z)\mathbf{n} = -\frac{\begin{bmatrix} G_1(z)C_1(z) & \cdots & G_1(z)C_m(z) \\ \vdots & \ddots & \vdots \\ G_m(z)C_1(z) & \cdots & G_m(z)C_m(z) \end{bmatrix}}{1 + \sum_{l=1}^{m} C_l(z)G_l(z)} \mathbf{n} \tag{3}$$

The steady state channel input power $\|\mathbf{y}\|_{Pow}^2 := \lim_{k\to\infty} \mathcal{E}\{\mathbf{y}^T[k]\mathbf{y}[k]\}$, with $\mathcal{E}\{\cdot\}$ the expectation, is known to satisfy in steady state the expression

$$\|\mathbf{y}\|_{Pow}^2 = \frac{1}{2\pi} \int_{-\pi}^{\pi} \mathrm{tr} \left(T^T\left(e^{j\omega}\right) \begin{bmatrix} \sigma_1^2 & \cdots & 0 \\ \vdots & \ddots & \vdots \\ 0 & \cdots & \sigma_m^2 \end{bmatrix} T\left(e^{j\omega}\right) \right) d\omega \tag{4}$$

where $\mathrm{tr}(\cdot)$ is the trace of a matrix. We then have that the overall channel input power satisfies

$$\mathcal{P} = \sum_{i=1}^{m} \mathcal{P}_i \geq \sum_{i=1}^{m} \sum_{j=1}^{m} \|T_{i,j}\|_2^2 \sigma_j^2 \tag{5}$$

with $T_{i,j}$ the i-th row, j-th column element of the matrix transfer function T defined in (3). Furthermore, if all the channel variances are equal, $\sigma_1^2 = \cdots = \sigma_m^2 = \sigma^2$, then we have

$$\frac{\mathcal{P}}{\sigma^2} \geq \sum_{i=1}^{m} \sum_{j=1}^{m} \|T_{i,j}\|_2^2 \tag{6}$$

The ratio $\frac{\mathcal{P}}{\sigma^2}$ can then be interpreted as the channel input SNR. We can now state the problem that we address in this work.

Problem 1: (**SNR problem**) Design the MISO controller $C(z)$ such that it stabilizes the closed feedback loop in Fig. 1, and that it also achieves a given value $\mathcal{P}_o$ for the channel input power, or equivalently Γ_o for the channel input SNR if $\sigma_i = \sigma$, for all i.

Remark 1: We observe that the channel input power constraint of each channel satisfies $\mathcal{P}_i \geq \sum_{j=1}^{m} \|T_{i,j}\|_2^2 \sigma_j^2$ that is, the SNR problem can also be studied for each channel separately. We also observe that the SIMO condition of the plant model limits the controller structure flexibility to solve Problem 1, since the same C_j is simultaneously affecting each $T_{i,j}$ with $j \neq i$, and, in turn, is affecting each channel input power $\mathcal{P}_i$ lower bound.

III. SNR Problem Solution for Stability and Asymptotic Tracking Performance

In this section we present our contributions that give solution to Problem 1. We start by considering a stabilizing controller solution, for the control feedback loop in Fig. 1, in the next theorem.

Theorem 1: **(Stabilizing SNR MISO Controller)** For the MISO controller

$$C = \begin{bmatrix} k_{c1} G_{s1}^{-1}(z) & \cdots & k_{cm} G_{sm}^{-1}(z) \end{bmatrix} \tag{7}$$

we design the controller gains k_{ci}, for $i = 1, \cdots, m$, such that, for each transfer function

$$T_{i,j}(z) = \frac{k_{cj} \prod_{\substack{l=1 \\ l \neq i}}^{m} (z - \rho_l)}{\prod_{l=1}^{m} (z - \rho_l) + \sum_{i=1}^{m} k_{ci} \prod_{\substack{l=1 \\ l \neq i}}^{m} (z - \rho_l)} \tag{8}$$

the common denominator satisfies

$$\prod_{l=1}^{m} (z - \rho_l) + \sum_{i=1}^{m} k_{ci} \prod_{\substack{l=1 \\ l \neq i}}^{m} (z - \rho_l) = \prod_{l=1}^{m} (z - 1/\rho_l) \tag{9}$$

from which we obtain numerically the values k_{ci}, which results in a stable closed feedback loop behavior. The overall channel input power will then be lower bounded by the expression

$$\mathcal{P} \geq \prod_{l=1}^{m} \rho_l^2 \sum_{i=1}^{m} \sum_{j=1}^{m} \frac{k_{cj}^2 \sigma_i^2}{\rho_i^2 - 1} \tag{10}$$

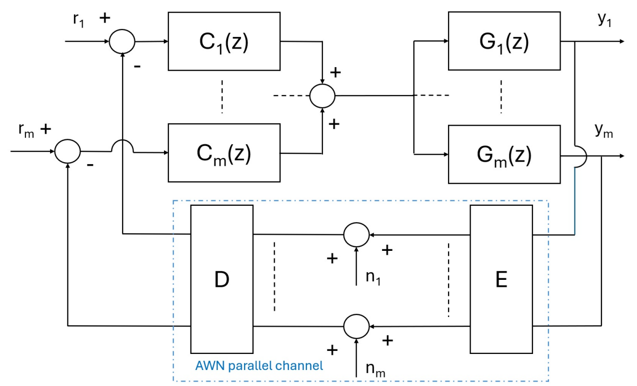

Fig. 2. NCS based on a set of AWN parallel channel over the feedback path, with encoder and decoder stages.

Proof: From Fig. 1 we have that the closed loop relationship, assuming $r_1 = \cdots = r_m = 0$, between the channel additive noise processes and the outputs is given by $\mathbf{y} = -\left(I + G(z)C(z)\right)^{-1} G(z)C(z)\mathbf{n}$. We then apply the Matrix Inversion Lemma and observe that

$$\begin{aligned} \mathbf{y} &= -\left[I - G(z)\left(1 + C(z)G(z)\right)^{-1} C(z)\right] G(z)C(z)\mathbf{n} \\ &= -G(z)\left(1 + C(z)G(z)\right)^{-1} \\ &\qquad \left[1 + C(z)G(z) - C(z)G(z)\right] C(z)\mathbf{n} \\ &= -\frac{G(z)C(z)}{1 + C(z)G(z)}\mathbf{n} \end{aligned} \tag{11}$$

which proves the expression presented earlier in (3) since the product $C(z)G(z)$ in the denominator is now scalar. We then replace the proposed plant and controller models in the above expression which reports (8) for each component of the matrix transfer function. From this point, we observe the resulting common denominator for each element in $T(z)$ and propose a pole assignment for a z-polynomial of degree m, with the controller gains k_{ci} as design parameters, such that the closed loop poles are located at the stable reflected positions $1/\rho_l$. This closed loop pole assignment is selected because it is well known that the minimum variance (or alternatively, minimum energy) controller design swaps the unstable pole locations to their reflected positions, see [6]. From this, we are left only with evaluating the resulting channel input power as in (5), through the H_2 norm of T induced by the proposed stabilizing controller. We then observe that in this case each element $T_{i,j}$ will result in

$$T_{i,j}(z) = \frac{k_{cj} \prod_{\substack{l=1 \\ l \neq i}}^{m} (z - \rho_l)}{\prod_{l=1}^{m} (z - 1/\rho_l)} = \frac{k_{cj} \prod_{l=1}^{m} \rho_l}{\rho_i z - 1} \frac{\prod_{\substack{l=1 \\ l \neq i}}^{m} (z - \rho_l)}{\prod_{\substack{l=1 \\ l \neq i}}^{m} (\rho_l z - 1)} \tag{12}$$

from which the right hand side of (10) is obtained, by observing that each term $\frac{z - \rho_l}{\rho_l z - 1}$ is all-pass and does not modify the resulting H_2 norm, which concludes this proof. ∎

Remark 2: We notice that the channel input power constraint stated in Equation (10) is under the assumption that the setpoint signals r_i, $i = 1, \cdots, m$ are set to zero. This is not a limitation for the result obtained in that the closed feedback loop is LTI, thus we can claim superposition, and in that stability is a property of the closed feedback loop, and it is not dependent on the external signals entering the loop.

We now present a corollary that focus on the case of a two-inputs single-output (TISO) controller to better visualize the previous theorem, and also clarify the design condition for each of the gain parameters k_{ci} in the controller.

Corollary 2: **(Stabilizing SNR TISO Controller)** For a SITO plant model with real, unstable poles ρ_1 and ρ_2, the gains k_{c1} and k_{c2}, of the related TISO controller, satisfy

$$k_{c1} = \frac{\left(\rho_1^2 - 1\right)\left(\rho_1\rho_2 - 1\right)}{\rho_1\rho_2\left(\rho_1 - \rho_2\right)}, \ k_{c2} = \frac{\left(\rho_2^2 - 1\right)\left(\rho_1\rho_2 - 1\right)}{\rho_1\rho_2\left(\rho_2 - \rho_1\right)} \tag{13}$$

and, if $\sigma_1^2 = \sigma_2^2 = \sigma^2$, then the channel input SNR is lower bounded by

$$\frac{\mathcal{P}}{\sigma^2} \geq \frac{\rho_1^2\rho_2^2\left(k_{c1}^2 + k_{c2}^2\right)\left(\rho_1^2 + \rho_2^2 - 2\right)}{(\rho_1^2 - 1)(\rho_2^2 - 1)} \tag{14}$$

Proof: Here we focus on the closed loop characteristic polynomial declared in (9) when $m = 2$. that is

$$z^2 + (-\rho_1 - \rho_2 + k_{c1} + k_{c2})z + \rho_1\rho_2 - k_{c1}\rho_2 - k_{c2}\rho_1 = z^2 - (\frac{1}{\rho_1} + \frac{1}{\rho_2})z + \frac{1}{\rho_1\rho_2}$$

In matrix form the above can be restated as

$$\begin{bmatrix} 1 & 1 \\ -\rho_2 & -\rho_1 \end{bmatrix} \begin{bmatrix} k_{c1} \\ k_{c2} \end{bmatrix} = \begin{bmatrix} -\frac{1}{\rho_1} - \frac{1}{\rho_2} + \rho_1 + \rho_2 \\ \frac{1}{\rho_1\rho_2} - \rho_1\rho_2 \end{bmatrix} \tag{15}$$

Inverting the known matrix on the left side results in the expressions for k_{c1} and k_{c2} reported in (13). The lower bound on the channel in put SNR stated in (14) is then a direct substitution of the gains in (13) into the expression in (10), deriving the lower bound for $\frac{\mathcal{P}}{\sigma^2}$, which concludes this proof. ∎

We are now required to satisfy the condition, by design, of an arbitrary power channel input $\mathcal{P}_o$. For this we extend the closed feedback loop to explicitly include an encoder/decoder stages, see Fig. 2. In the next theorem we offer the design of such stages to achieve our objective.

Theorem 3: **(Encoder/Decoder design for a desired channel input power $\mathcal{P}_o$)** Based on the controller design from Theorem 1, the encoder and decoder in Fig. 2, in order to achieve a given value $\mathcal{P}_o$, are given by

$$E = \begin{bmatrix} \sqrt{\frac{m\left(\sum_{i=1}^m \|T_{i,1}\|_2^2\right)\sigma_1^2}{\mathcal{P}_o}} & \cdots & 0 \\ \vdots & \ddots & \vdots \\ 0 & \cdots & \sqrt{\frac{m\left(\sum_{i=1}^m \|T_{i,m}\|_2^2\right)\sigma_m^2}{\mathcal{P}_o}} \end{bmatrix} = D^{-1} \tag{16}$$

Proof: The presence of the encoder and the decoder stages results in a closed loop relationship between $\mathbf{y}$ and $\mathbf{n}$ given by $\mathbf{y} = -\frac{G(z)C(z)}{1+C(z)G(z)}D\mathbf{n}$. We then observe that d_i, the elements in the diagonal of D, are numbers not transfer functions, and thus the overall channel input lower bound, with the stabilizing controller designed as in Theorem 1, is

$$\Sigma = \sum_{i=1}^m \left(\sum_{j=1}^m \|T_{i,j}\|_2^2\right) d_i^2\sigma_i^2 \tag{17}$$

We then replace $d_i^2 = \frac{\mathcal{P}_o}{m\left(\sum_{i=1}^m \|T_{i,m}\|_2^2\right)\sigma_m^2}$ from (16) which results in $\Sigma = \mathcal{P}_o$, which concludes this proof. ∎

Remark 3: We observe here that if $\mathbf{r}$ is not zero, then a positive extra term, say Φ_o, will be added to the overall channel input power. Nevertheless, any increase due to the setpoint signals can be reverted by appropriately choosing the desired channel input power to be $\mathcal{P}_o - \Phi_o$ (as long as $\mathcal{P}_o$ is greater than Φ_o), instead of just $\mathcal{P}_o$.

We proceed in the next corollary to illustrate the encoder and decoder designs, for the special case of $m = 2$, for which they turn to be two-inputs two-outputs (TITO) systems.

Corollary 4: **TITO Encoder/Decoder design for Γ_o** For a SITO plant model with real and unstable poles ρ_1 and ρ_2, the TISO controller gains k_{c1} and k_{c2} designed as in Corollary 2, the encoder/decoder designs to achieve a given power channel $\mathcal{P}_o$ are

$$E = \begin{bmatrix} \sqrt{\frac{2\left(\|T_{1,1}\|_2^2 + \|T_{2,1}\|_2^2\right)\sigma_1^2}{\mathcal{P}_o}} & 0 \\ 0 & \sqrt{\frac{2\left(\|T_{1,2}\|_2^2 + \|T_{2,2}\|_2^2\right)\sigma_2^2}{\mathcal{P}_o}} \end{bmatrix} = D^{-1} \tag{18}$$

Proof: The proof of this corollary is by direct application of Theorem 3 for $m = 2$, which concludes this proof. ∎

We now introduce, on top of the stabilization achieved by the controllers C_i, the design of a feed forward matrix F, in order to achieve asymptotic tracking of constant setpoints.

Theorem 5: **(Asymptotic Tracking Performance)** To achieve asymptotic tracking of constant setpoints, we introduce a feed forward matrix F as depicted in Fig. 3. The design of such an F to achieve asymptotic tracking is given by

$$F = I - T(1) \tag{19}$$

Proof: The fact that the closed feedback loop in Fig. 3 is LTI allow for superposition. More so the fact that the noise processes are zero mean implies that we can focus only on the closed loop relationship between $\mathbf{y}$ and $\mathbf{r}$. Notice also from Fig. 3 that $\mathbf{y} = \mathbf{w} + F\mathbf{r} = T(z)\mathbf{r} + (I - T(1))\mathbf{r}$ As $z \to 1$, for asymptotic tracking, we then retrieve $\mathbf{y} \to \mathbf{r}$, which concludes the proof. ∎

We have presented, in this section, step by step the designs of the different elements of the closed feedback loop in Fig. 3 that solve Problem 1. In the next section we illustrate these results with an example.

IV. Examples

In this section we present an example to highlight the contributions from the previous section. We consider a TISO

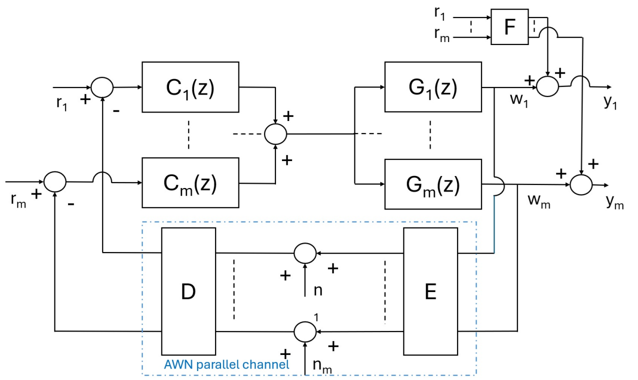

Fig. 3. NCS based on a set of AWN parallel channel over the feedback path, with encoder and decoder stages, and asymptotic tracking.

plant model given by

$$G(z) = \begin{bmatrix} \frac{1}{z-3} & \frac{1}{z-4} \end{bmatrix}^T \tag{20}$$

where we recognize $\rho_1 = 3$, and $\rho_2 = 4$. As each element of the SITO plant model does not contain an explicit stable, minimum phase, biproper $G_{si}(z)$ term, then the TISO stabilizing controller resulting from the use of Corollary 2 is directly the pair of gains k_{c1} and k_{c2}

$$C = \begin{bmatrix} k_{c1} & k_{c2} \end{bmatrix} = \begin{bmatrix} -7.3333 & 13.75 \end{bmatrix} \tag{21}$$

The resulting expression for the closed feedback loop is then

$$T(z) = \begin{bmatrix} \frac{-7.3333(z-4)}{(z-0.3333)(z-0.25)} & \frac{13.75(z-4)}{(z-0.3333)(z-0.25)} \\ \frac{-7.3333(z-3)}{(z-0.3333)(z-0.25)} & \frac{13.75(z-3)}{(z-0.3333)(z-0.25)} \end{bmatrix} \tag{22}$$

We now assume that the zero mean noise processes for each channel have equal variance σ^2, and when required, numerically equal to 0.1. For the matrix transfer function above the channel input SNR $\mathcal{P}/\sigma^2$ is lower bounded, as predicted by Theorem 1, by

$$\frac{\mathcal{P}}{\sigma^2} \geq 6702.4 \Rightarrow 38.2623 \ (dB) \tag{23}$$

We study the sensitivity of the resulting SNR lower bound as function of k_{c1} in Fig. 4, when $k_{c2} = 13.75$, and as function of k_{c2}, when $k_{c1} = -7.3333$, in Fig. 5. We observe that, as predicted by Theorem 1, we are achieving said lower bound, blue dashed lines, and such a value has been correctly predicted as $38.2623 \ dB$. We now propose, through the use of Corollary 4, the choice of achieving a target channel input SNR $\mathcal{P}_o/\sigma^2$ of

$$\frac{\mathcal{P}_o}{\sigma^2} = \rho_1^2\rho_2^2 - 1 = 143 \Rightarrow 21.5534 \ (dB) \tag{24}$$

For the above Γ_o, the encoder and decoder stages have to be selected as

$$E = \begin{bmatrix} 4.5562 & 0 \\ 0 & 8.5429 \end{bmatrix}, \quad D = \begin{bmatrix} 0.2195 & 0 \\ 0 & 0.1171 \end{bmatrix} \tag{25}$$

We observe that Theorem 3, and thus Corollary 4, do not modify the designed TISO stabilizing controller presented

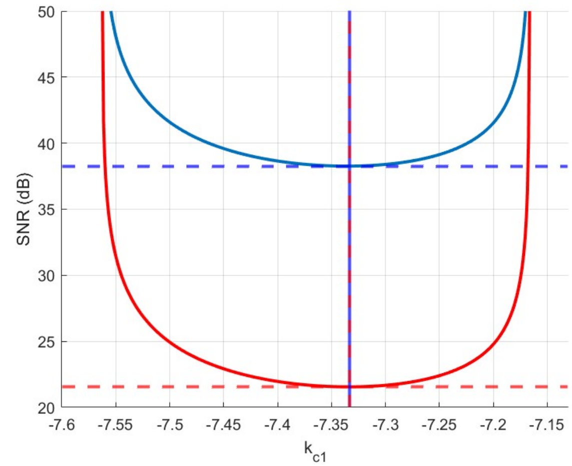

Fig. 4. Resulting SNR with the stabilizing controller as function of k_{c1}. Theorem 1, blue solid line, Corollary 4, red solid line.

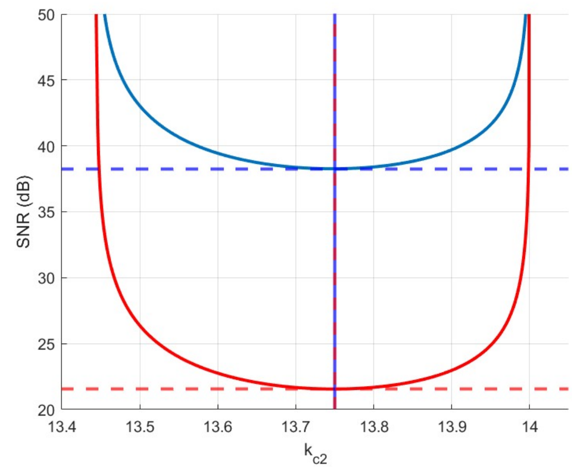

Fig. 5. Resulting SNR with the stabilizing controller as function of k_{c2}. Theorem 1, blue solid line, Corollary 4, red solid line.

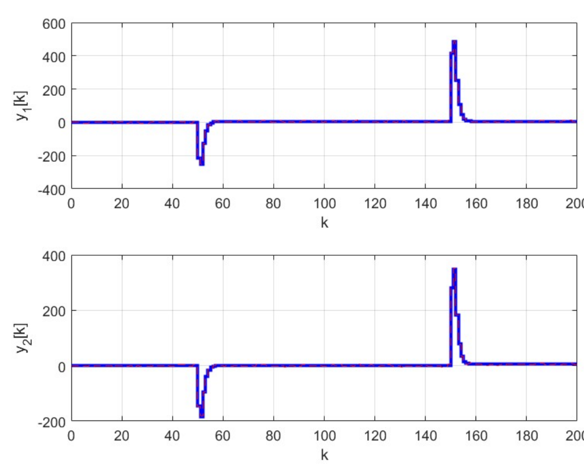

Fig. 6. Output signals asymptotic tracking. Setpoint r_1 step function of size 5 applied at $k = 50$. Setpoint r_2 step function of size 5 applied at $k = 150$.

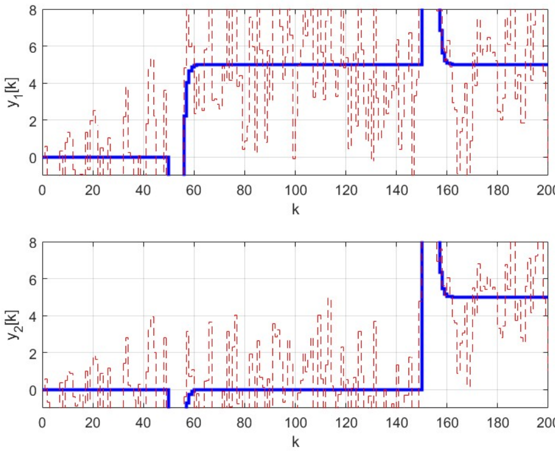

Fig. 7. Zoom in on both output signals, y_1 and y_2, to verify the asymptotic tracking

in (21). With such a stabilizing controller solution and the encoder/decoder design in (25) we perform a similar controller gains sensitivity analysis. As already reported in Figs. 4 and 5 in red color, we maintain the controller in (21) and also satisfy the selected lower bound of $\mathcal{P}_o/\sigma^2 = 21.5534$ in decibels, red dashed lines.

We now consider Theorem 3 to achieve asymptotic tracking of constant setpoint signals. The resulting feed forward gain matrix is then

$$F = \begin{bmatrix} -43 & 82.5 \\ -29.3333 & 56 \end{bmatrix} \tag{26}$$

We explore the resulting tracking for r_1 a step signal of amplitude 5, applied at $k = 50$, and r_2 also as a step signal of amplitude 5, but applied at $k = 150$. The noise variance for each channel is selected to be $\sigma^2 = 0.1$. In Fig. 6 we present y_1 and y_2 as in Fig. 3. We see that, due to the interaction of the values of ρ_1 and ρ_2 into $T(z)$ in (22) we have strong couplings, with large excursions of both signals in each case. To further verify the achieved asymptotic tracking we present a zoom in of the achieved output signals trajectories in Fig. 7. The blue solid lines represent the case of no noise, from which we verify the achieved objective after the closed feedback loop achieves steady state, first for y_1, and then for y_2. The noisy versions of both output signals are reported in red dashed line and it can be observed that they are centered on the predicted noiseless trajectories due to the zero mean characteristic of each additive channel noise. Finally, although the results developed here are not comparable with [14], or [15], since those results are in continuous time and deal with the error performance and not the channel SNR, we would expect that any added communication feature (packet dropout, quantization, etc.) will further increase the presented SNR limitations.

We have then explored in this section all the theoretical contributions proposed in Section III.

V. Conclusions

In this article, we investigated a networked control system architecture based on a set of parallel AWN channels in the feedback path, operating under a global power constraint. The plant considered was a SIMO LTI system. As a direction for future work, this analysis should be extended next to multi-input multi-output (MIMO) configurations with a lower number of inputs than outputs. For the SIMO plant model addressed in this study, we first developed a stabilizing controller for the closed-loop feedback configuration. We then enhanced this stabilizing solution by introducing encoder and decoder stages, enabling the enforcement of an arbitrary bound on the channel input power. Finally, we incorporated a feedforward gain for the setpoint signals to guarantee asymptotic setpoint tracking of the closed-loop output signals.

References

[1] R. P. Borase, D. K. Maghade, S. Y. Sondkar, and S. N. Pawar, “A review of PID control, tuning methods and applications,” *International Journal of Dynamics and Control*, vol. 9, pp. 818–827, 2021.

[2] W. S. E. Levine, *The Control Handbook*. CRC Press, 1996.

[3] M. J. Blondin, J. S. Saez, and P. M. Pardalos, “Control Engineering from Classical to Intelligent Control Theory—An Overview,” *Springer optimization and its applications*, vol. 1, pp. 1–30, 2019.

[4] X. Zhang, Q. Han, and X. Yu, “Survey on Recent Advances in Networked Control Systems,” *IEEE Transactions on Industrial Informatics*, vol. 12, pp. 1740–1752, 2016.

[5] G. Nair and R. Evans, “Stabilizability of stochastic linear systems with finite feedback data rates,” *SIAM J. Control and Optimization*, vol. 43, no. 2, pp. 413–436, July 2004.

[6] J. Braslavsky, R. Middleton, and J. Freudenberg, “Feedback Stabilisation over Signal-to-Noise Ratio Constrained Channels,” *IEEE Transactions on Automatic Control*, vol. 52, no. 8, pp. 1391–1403, 2007.

[7] X. Ge, F. Yang, and Q. Han, “Distributed networked control systems: A brief overview,” *Information Sciences*, vol. 380, pp. 117–131, 2017.

[8] X. Zhang, Q. Han, X. Ge, D. Ding, L. Ding, D. Yue, and C. Peng, “Networked control systems: a survey of trends and techniques,” *IEEE/CAA Journal of Automatica Sinica*, vol. 7, pp. 1–17, 2020.

[9] J. Østergaard, “Stabilizing Error Correction Codes for Controlling LTI Systems over Erasure Channels,” *IEEE Transactions on Control on Network Systems*, vol. 9, pp. 1828–1839, 2022.

[10] C. Tan, H. Zhang, W. Wong, and Z. Zhang, “Feedback Stabilization of Uncertain Networked Control Systems Over Delayed and Fading Channels,” *IEEE Transactions on Control of Network Systems*, vol. 8, pp. 260–268, 2021.

[11] X. Litrico, “Robust IMC flow control of SIMO dam-river open-channel systems,” *IEEE Trans. Control. Syst. Technol.*, vol. 10, pp. 432–437, 2002.

[12] X.-W. Jiang, C. Chen, Q. Yang, X. Qu, and H. Yan, “Optimal tracking performance for SIMO systems with packet dropouts and control energy constraints,” *IET Control Theory & Applications*, vol. 12, pp. 1714–1721, 2018.

[13] X. Hu, X. Zhan, J. Wu, and H. Yan, “Performance of SIMO Networked Time-Delay Systems With Encoding–Decoding and Quantization Constraints,” *IEEE Access*, vol. 8, pp. 55 125–55 134, 2020.

[14] L. Cheng, H. Yan, X. Zhan, and C. Yuan, “Performance Analysis of SIMO Networked Control Systems Under Quantization and Packet Dropout,” in *China Automation Congress (CAC)*, Beijing, China, October 2021, pp. 8262–8266.

[15] C. Chen, F. Liu, L. Wu, H. Yan, W. Gui, and H. Stanley, “Tracking Performance Limitations of Networked Control Systems With Repeated Zeros and Poles,” *IEEE Transactions on Automatic Control*, vol. 66, pp. 1902–1909, 2021.

[16] A. J. Rojas, “Signal-to-Noise Ratio Input Constrained Control of Single- Input Multiple-Output Systems,” *IEEE Transactions on Control of Network Systems*, vol. 12, pp. 2372–2380, 2025.